Knudsen Cell Studies of the Reaction of Gaseous HNO_3 with NaCl Using Less than a Single Layer of Particles at 298 K: A Modified Mechanism

Rachel C. Hoffman, Margaret A. Kaleuati, and Barbara J. Finlayson-Pitts*

Department of Chemistry, University of California, Irvine, California 92697-2025

Received: May 12, 2003; In Final Form: July 24, 2003

The uptake and reaction of HNO_3 with NaCl was studied at 298 K using a Knudsen cell coupled to a quadrupole electron impact mass spectrometer. Experiments were conducted using less than one layer of particles to clearly define the available reactive surface area. The uptake of HNO_3 was observed to be faster initially than at longer reaction times. A new model is proposed that incorporates reactions at two different types of sites: (1) steps and edges on the NaCl surface holding surface adsorbed water (SAW) and (2) dry terrace sites. The initial, more rapid uptake is attributed to reaction with both types of sites on a fresh NaCl surface, while the slower uptake at longer reaction times is due only to reaction at the steps and edges where new reaction sites are generated by the SAW-assisted recrystallization of the $NaNO_3$ product. The initial uptake coefficient based on data at short reaction times is $\gamma^0 = (2.3 \pm 1.9) \times 10^{-3}$, in agreement within the experimental errors with a value of $\gamma^0 = (1.1 \pm 0.4) \times 10^{-3}$ (2s) derived from the dependence of the uptake coefficient on the initial HNO_3 concentration. The fraction of the surface area covered by sites holding SAW was estimated to be approximately 50% based on the uptake coefficient, averaged over three cycles of exposure to HNO_3, $\gamma = (1.0 \pm 0.8) \times 10^{-3}$ (2s). The data suggest that the reaction of HNO_3 with effluoresced sea salt particles is less important than previously thought relative to reactions with N_2O_5 and $ClONO_2$, which generate chlorine atom precursors.

I. Introduction

Heterogeneous reactions involving sea salt aerosol rich in NaCl, which are dispersed into the troposphere through wind and wave action of the oceans,[1] could contribute to the overall tropospheric halogen budget. The reaction of sea salt aerosols with HNO_3 generates photochemically inert hydrochloric acid (HCl) in contrast to the reaction with N_2O_5 and $ClONO_2$, which yields photochemically active chlorine-containing compounds[2−37]

$$HNO_{3\,(g)} + NaCl_{(s)} \rightarrow NaNO_{3\,(s)} + HCl_{\,(g)} \quad (1)$$

$$N_2O_{5\,(g)} + NaCl_{\,(s)} \rightarrow NaNO_{3\,(s)} + ClNO_{2\,(g)} \quad (2)$$

$$ClONO_{2\,(g)} + NaCl_{\,(s)} \rightarrow NaNO_{3\,(s)} + Cl_{2\,(g)} \quad (3)$$

These reactions (1−3) may contribute to the observed chloride deficits in sea salt particles in the marine boundary layer (MBL) of polluted coastal regions.[38−43] To better understand the contribution of these reactions to the halogen budget, this study focuses on uptake and reaction of HNO_3 (reaction 1).

Table 1 summarizes a number of previous studies of reaction 1 conducted using several different techniques. Hydrochloric acid is the sole gaseous product from reaction 1 with a 100% yield.[11,16,18,19,28] The reported uptake coefficients (γ), however, span 2 orders of magnitude, making it difficult to evaluate the importance of reaction 1 relative to reactions 2 and 3, which lead to photochemically active products.

There are a number of potential reasons for the discrepancies in the reported uptake coefficients. The most important issue is a lack of accurate knowledge of the available reactive surface area. When multiple layers of particles are used, the gaseous HNO_3 can diffuse between the salt particles into lower layers, increasing the available reactive surface area compared to the commonly used geometric area of the sample holder. This issue of diffusion into the salt sample in Knudsen cell studies has been discussed by a number of researchers.[11,16,18,19,28,44−48] In the limit of very fast reactions ($\gamma \rightarrow 1$), the gas is taken up before it can diffuse into the pores of the powder, and the geometric surface area is a good approximation. In very slow reactions, the gas can diffuse throughout the layers; in this case, the entire salt surface area is available for reaction, leading to a smaller calculated uptake coefficient than that using the geometric area. Both of these extremes are readily addressed in obtaining calculated uptake coefficients. However, when diffusion occurs only into the top few layers of the sample, estimating the true available reactive surface is more difficult.

Another issue affecting the reactive surface area is the formation of the product $NaNO_3$ on top of the NaCl, leading to saturation of the surface. This was observed by Laux et al.,[8] Leu et al.,[16] and Zangmeister and Pemberton.[34] Davies and Cox[28] observed a dependence of γ on the HNO_3 concentration, which they attributed to surface saturation. To explain the dependence, Davies and Cox proposed a two-site model in which HNO_3 is adsorbed on the salt surface with subsequent surface diffusion to defect sites that contain adsorbed water, where the reaction with chloride occurs. Ghosal and Hemminger[31] developed a single-site Langmuir model to explain their initial uptake coefficient for the fresh single-crystal NaCl surface of $(1.3 \pm 0.6) \times 10^{-3}$, in which HNO_3 reacts with an NaCl site to form surface nitrate. The thin surface nitrate product layer is mobilized by water into microcrystallites of $NaNO_3$ attached to the surface, regenerating a fresh NaCl surface. The uptake

* To whom correspondence should be addressed. Phone (949) 824-7670. FAX (949) 824-3168. E-mail: bjfinlay@uci.edu.

10.1021/jp030611o CCC: $25.00
Published on Web 09/03/2003

TABLE 1. Summary of the Previous Studies on the Reaction of HNO_3 with Solid NaCl

NaCl type	ref	γ at 298 K	comments	technique
single crystal	Laux et al., 1994	$(4 \pm 2) \times 10^{-4}$	surface saturation by $NaNO_3$	XPS/UHV
ground powders	Fenter et al., 1994	$(2.8 \pm 0.3) \times 10^{-2}$	independent of salt size and amount	Knudsen cell/MS
powders	Leu et al., 1995	$(1.3 \pm 0.4) \times 10^{-2}$	corrected γ using a pore diffusion model[71,72]	flow system/MS
ground powders, single crystals, and spray-coated films	Fenter et al., 1996	$(2.0 \pm 1.0) \times 10^{-2}$	independent of salt size and amount	Knudsen cell/MS
ground powders and single crystals	Beichert and Finlayson-Pitts, 1996	$(1.4 \pm 0.6) \times 10^{-2}$	independent of $[HNO_3]$ from $(3-35) \times 10^{12}$ molecules cm^{-3}, number of particle layers, and particle size; surface adsorbed water important in uptake and reaction	Knudsen cell/MS
ground powders	Davies and Cox, 1998	$(0.8-9) \times 10^{-4}$	dependence on $[HNO_3]$ from $(0.5-70) \times 10^{12}$ molecules cm^{-3}	flow system/MS
spray-coated films	Koch et al., 1999	$(4.0 \pm 1.0) \times 10^{-2}$	precursor-mediated adsorption	molecular diffusion tube
ground powders and single crystals	Ghosal and Hemminger, 1999	$(1.3 \pm 0.6) \times 10^{-3}$	predicted model value to explain HNO_3 dependence; applied to Davies and Cox data to get $\gamma^0 = 1.1 \times 10^{-3}$	XPS/UHV
recrystallized NaCl	Zangmeister and Pemberton, 2001	$(5.9 \pm 0.8) \times 10^{-2}$	detection of $NaNO_3$ microcrystallites	Raman spectroscopy
single crystals	Ghosal and Hemminger, 2002	$\leq (5 \pm 3) \times 10^{-3}$	observed SAW on defects sites of 1−10-μm NaCl powders and to a lesser extent, on 500-μm particles.	XPS/UHV

coefficient for HNO_3 was predicted to be related to the amount of water present and the HNO_3 concentration. This was shown to be consistent with the Davies and Cox[28] data for which a value of $\gamma^0 = 1.1 \times 10^{-3}$ for the maximum uptake coefficient at high water concentrations was derived.

We report studies of the reaction of HNO_3 with NaCl powders that provide sufficient steps, edges, and defects known to hold SAW, which plays an important role in the chemistry of the atmosphere. These salt particles of known sizes were spread on the sample holder in amounts less than a single layer. This avoids the issue of diffusion into multiple salt layers. In addition, the time-dependence of the uptake coefficient provides insight into the issue of saturation of the surface during the reaction. We propose a new reaction model in which there are two types of reaction sites. The atmospheric implications of this reaction are discussed.

II. Experimental Methods

Reaction 1 was studied using a glass Knudsen cell coupled to a quadrupole electron impact mass spectrometer described in detail elsewhere.[19,49,50] Briefly, the cell is equipped with a moveable lid to cover or expose salt samples within a sample holder positioned on a stainless steel platform. Reactant gases entered the cell from a glass manifold via a stainless steel needle valve. The needle valve and all components of the Knudsen cell were coated with halocarbon wax (Halocarbon Products, Series 1500) which has been found to be inert to HNO_3. The salt samples were placed in a halocarbon wax-coated stainless steel holder having a geometric surface area of 19.0 cm^2. Most experiments were conducted at HNO_3 concentrations ranging from $(2-6) \times 10^{11}$ molecules cm^{-3}. Additional experiments were carried out at higher HNO_3 concentrations ($0.5-8 \times 10^{13}$ molecules cm^{-3}) to probe for the dependence of the uptake coefficient on the HNO_3 pressure that was reported in some previous studies.[16,28]

The reactant and/or product gases exit the Knudsen cell through a halocarbon wax-coated glass aperture (3.8 mm diameter) into a dual differentially pumped vacuum chamber quadrupole mass spectrometer (ABB Extrel EMBA II 150-QC) with electron impact ionization. The ion current signal was interfaced through a preamplifier to a computer with data acquisition capabilities (ABB Extrel, Merlin, Rev. B). The species monitored were HNO_3 ($m/z = 30$, 46 and 63) and HCl ($m/z = 36$ and 38). Quantification was based on the NO_2^+ ($m/z = 46$) and/or HCl^+ ($m/z = 36$) signals, which had the highest intensities. The instrument sensitivity was optimized for the fractional salt layer experiments, resulting in typical detection limits (2s) for HNO_3 and HCl of 5×10^9 and 2×10^9 molecules cm^{-3}, respectively. All uptake studies were carried out at 298 K. Upon initiation of each experiment, salt samples were placed in the Knudsen cell and pumped on for several minutes. Without heating or extensive pumping, SAW will be present on these salt samples.

Experimental Description. NaCl powders and single crystals were obtained from Fluka (> 95.5%) and Reflex, respectively. Varying sample sizes were obtained either by sieving the powders as received or by sieving and crushing single crystal samples. Sieves (U. S. Standard) used included #20, 35, 40, 60, and 120, which retain salt sizes of roughly 850, 500, 425, 250, and 125 μm, respectively.

Scanning electron microscopy (SEM) images of three sputter-coated NaCl salt samples show a typical cubic shape for the sieved powders (Figure 1). Averages sizes were calculated to be 177 ± 76, 290 ± 111, and 439 ± 99 μm (2s), determined using the length and width of a representative sample of particles. Individual salt particles contain steps, edges, and defects in addition to flat terrace regions. Figure 2, for example, shows a particle that has more than the usual amount of surfaces features to demonstrate this aspect of the surface. While Figure 2 illustrates that not all particles are atomically flat, NaCl powders have been shown[13,16] to be nonporous. In addition, the surface area of NaCl powders calculated using SEM images were shown to be in agreement with BET surface areas. Those determined using SEM, however, are more accurate and hence, are used here.

Crushed salt samples were also used for comparison to sieved powders. These crushed particles were found to have asymmetrical dimensions and irregular shapes and surfaces (Figure 3). The average size was calculated from the length and width of a typical sample to be 164 ± 102 μm (2s). Although the particles displayed irregular shapes, a cubic geometry was assumed with the same average surface area per side as

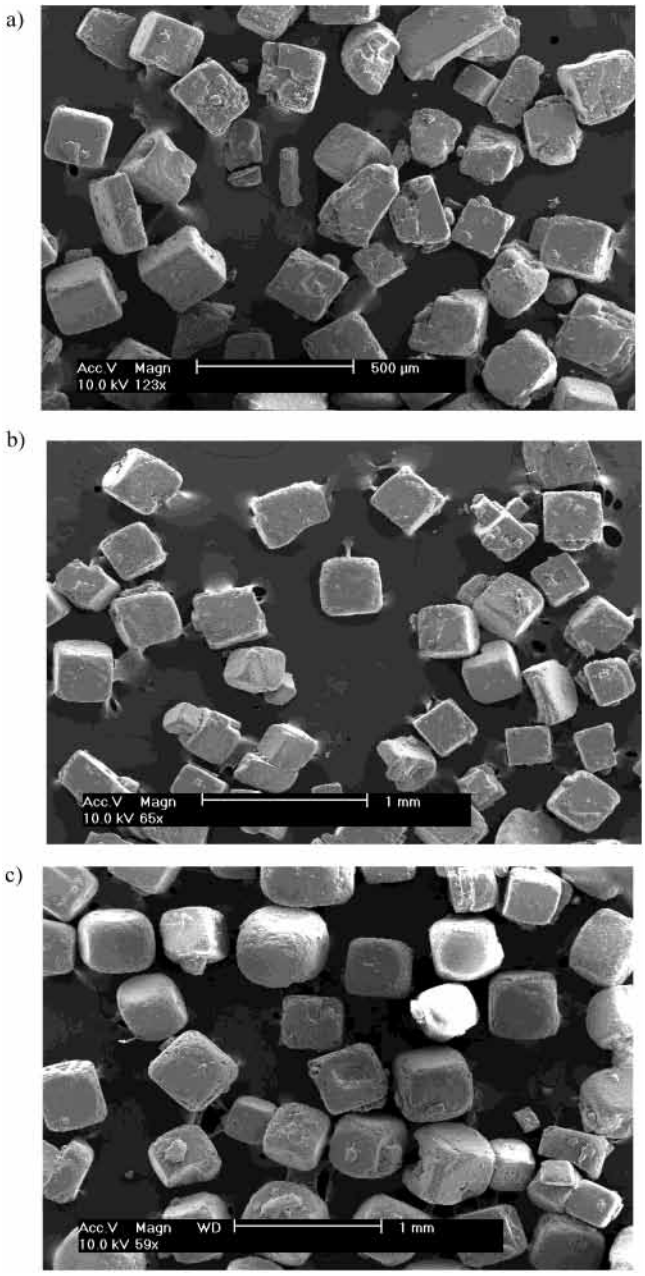

Figure 1. SEM images of three sieved NaCl powder samples. (a) 177 ± 76 μm, (b) 290 ± 111 μm, and (c) 439 ± 99 μm (2s).

measured from the tops of the irregularly shaped crystals. A more accurate average size could not be obtained using three sides of each particle due to the inaccuracies in measuring the height of the particles from the SEM images.

To determine the number of fractional particle layers, the total volume of the salt was calculated using the density of NaCl, 2.165 g cm^{-3}, and the mass of the sample. The volume per particle was calculated from the average SEM dimensions and used to determine the total number of particles. The fraction of a layer of salt was calculated from the portion of the geometrical surface area of the sample holder that was covered by the surface of the particles.

A few multiple layer experiments were conducted to demonstrate the effect of using the geometrical surface area of the sample holder in determining the uptake coefficient. The number of layers in the multiple layer experiments was calculated by $(m/\rho_b A_{geom} h)$, where m is the mass of the salt sample, ρ_b is the bulk density of the salt, A_{geom} is the geometric surface area of the sample holder, and h is the height of one salt particle. The bulk density takes into account the openings between salt particles and was determined using the volume of the sample holder and the amount of salt to losely fill it. The bulk density for the 177-μm particles used was measured to be 1.3 g cm^{-3}.

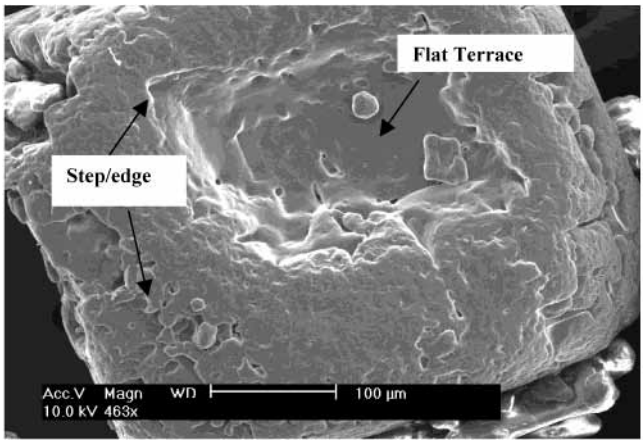

Figure 2. Close-up SEM image of a typical 439 μm NaCl particle showing numerous steps, edges, and defects.

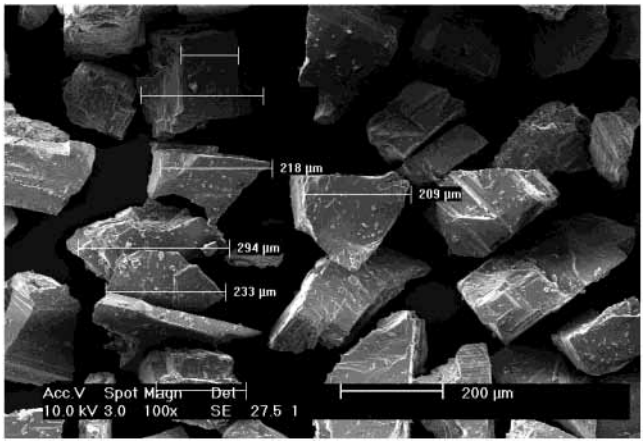

Figure 3. SEM image of 164 ± 102 μm (2s) NaCl prepared from crushed, sieved single crystals.

Chemicals. Dry HNO_3 was extracted from the vapor over a solution of concentrated HNO_3 and H_2SO_4 (1:2 v/v) and either used directly or mixed with He (Oxygen Service, 99.9995%) to obtain lower HNO_3 concentrations. Concentrated HNO_3 (Fisher, 69.7 wt. %), H_2SO_4 (Fisher, 96.0 wt. %) and HCl gas (Scott Specialty Gases, 99.995%) were used as obtained.

Calculation of Uptake Coefficients. The details of Knudsen cell experiments have been discussed in detail elsewhere.[11,20,51−54] In brief, gas molecules may leave the reaction chamber through the exit aperture or be removed by collision, uptake, and/or reaction with the sample surface. The measured uptake coefficient, γ_{meas}, is determined by the ratio of the loss of reactant gas molecules through the exit aperture to the loss on the salt surface

$$\gamma_{meas} = \left(\frac{I_o}{I_r} - 1\right)\left(\frac{A_{aperture}}{A_{surface}}\right) \qquad \text{(I)}$$

where I_o and I_r are the reactant signals in the absence and presence of a reactive surface, respectively, $A_{aperture}$ is the area of the exit aperture from the Knudsen cell to the mass spectrometer, and $A_{surface}$ is the reactive surface area of the salt sample.

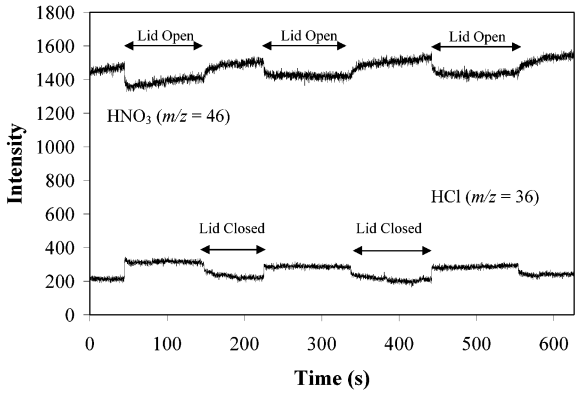

Figure 4. Uptake of HNO_3 and production of HCl for 0.3 particle layers of 290 μm NaCl particles that had been pumped on for several minutes at room temperature (experiment #20). Initial $[HNO_3]_0 = 4.9 \times 10^{11}$ molecules cm^{-3}.

In our preliminary calculations, $A_{surface}$ was taken for convenience to be the geometric surface area of the sample holder (19.0 cm^2). The uptake coefficient calculated using the geometric surface area is denoted as γ_{geom}. As described in more detail below, this was corrected to reflect the true available surface for the fractional particle layer experiments, denoted as γ_{corr}.

Uncertainties in the values of the uptake coefficients using less than one layer of NaCl arise from several sources. First, using crushed, sieved, single-crystal salt samples, there is uncertainty in the average particle size; the particles are treated as cubic and uniform in size for application of the model described below for the fractional particle layer experiments. While using the cubic, sieved powders eliminates some of this uncertainty, there is still a range of sizes for each sample. A 25% uncertainty in the size of the particles yields an error in the uptake coefficient of ~15% for the fractional particle layer experiments. Second, we assume that the particles are evenly distributed on the sample holder in calculating the fraction of the sides available for reaction. This appeared visually to be a reasonable approximation. Finally, these experiments were intentionally carried out on salts that had not been extensively pumped on, to maximize the amount of SAW present. The amount of SAW, however, may vary from sample to sample due to variations in steps, edges, and defects on which the water is believed to be adsorbed.[32,55−61]

The experimental errors reported were determined in two ways. The error for individual experiments was estimated using a propagation of errors for the raw signals and their measured variability. The errors for the average uptake coefficients are two standard deviations (2s) of the mean.

III. Results and Discussion

Figure 4 shows typical data for the loss of HNO_3 and generation of HCl for reaction on less than one layer of NaCl salt. Typically, there is a more rapid uptake and reaction of HNO_3, as well as production of HCl, when the lid is first opened, as observed in our earlier multilayer studies[19] and by previous researchers.[11,28] HCl is observed as the sole product. The initial uptake of HNO_3 was typically larger than that after several cycles of opening and closing the lid to expose the sample to HNO_3. We report below two values for the uptake coefficient, one at short reaction times (<10 s), γ^0, and one at larger reaction times, γ, chosen for consistency to be at the end of the third cycle of opening and closing the sample lid.

Figure 5 shows uptake coefficients at longer reaction times as a function of the particle layers from 0.5 to 12 layers. It is seen that the value of γ_{geom}, calculated using the geometric surface area of the sample holder, increases with increasing particle layers, suggesting that diffusion into the salt sample is important and that more than the geometric surface area is available for reaction.

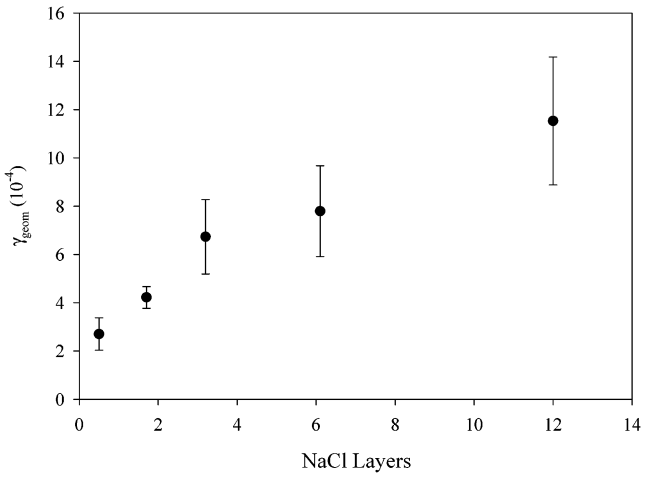

Figure 5. Uptake coefficients for a geometric reactive surface area (γ_{geom}) as a function of the number of particle layers for 177 μm NaCl particles.

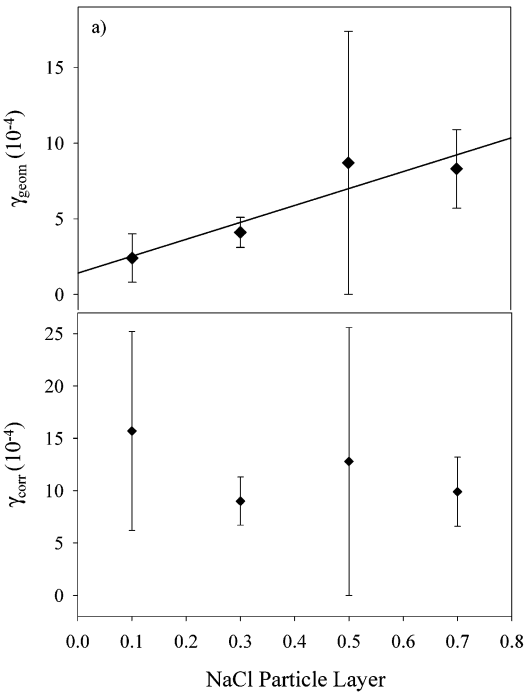

Figure 6. (a) Uptake coefficients assuming the geometric reactive surface (γ_{geom}) as a function of the fraction of a particle layer of 439 μm NaCl particles for initial HNO_3 concentrations of $\sim 5 \times 10^{11}$ molecules cm^{-3}; (b) Uptake coefficients for a true reactive area (γ_{corr}) as a function of the fraction of a single particle layer for the 439 μm NaCl particles shown in (a). Error bars represent two standard deviations of the mean for multiple experiments.

Figure 6a shows γ_{geom} as a function of the fraction of a salt layer. Here, the impacts of diffusion are eliminated, as diffusion into underlying layers is not possible. Under these conditions, the true available reactive surface area can be calculated with reasonable accuracy based on the particle sizes measured using SEM and the knowledge that the salt particles are not porous,[13,16] using a model previously developed in this laboratory.[37] The portion of the salt particles available for reaction includes the tops as well as a fraction of the sides of the particles. The total

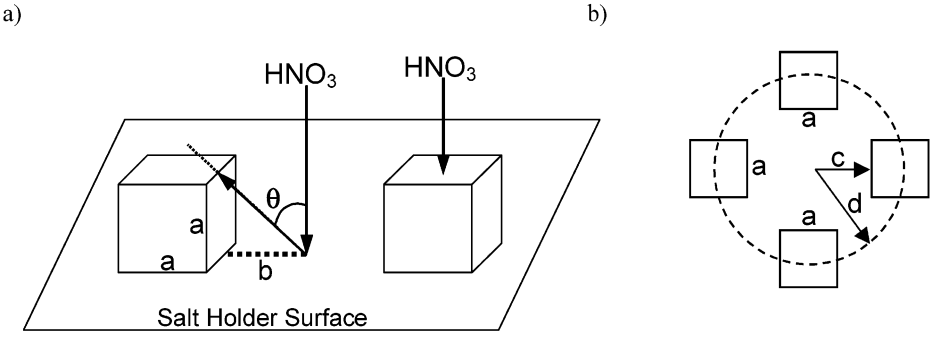

Figure 7. (a) Diagram of scattering of HNO_3 molecules that hits the bottom of the sample holder and collide with the side of a NaCl particle, and (b) circle used to calculate "holes" between salt particles, showing HNO_3 scattering trajectories that strike an NaCl particle (*c*) and that pass between particles (*d*).

top area can be calculated from the dimensions obtained from the SEM images and the total number of particles. However, if an incoming HNO_3 molecule strikes an open space (hole) between particles, it will be scattered off the bottom of the sample holder. In this case, it will either be scattered away from the surface, never coming in contact with a NaCl particle or, if at an appropriate angle, it may strike a side of a nearby NaCl particle (Figure 7a). The fraction of HNO_3 molecules that strike a particle side will be determined by the proximity of particles to each other and the scattering angle. On the basis of the size of the crystals and the distance between them, the angle, θ, can be calculated from eq II

$$\theta = 90 - \arctan\frac{a}{b} \qquad \text{(II)}$$

where *a* is the height of a salt particle and *b* is half the distance between two particles. It is assumed that an HNO_3 molecule strikes the sample holder surface equidistant from evenly spaced NaCl particles.

The fraction of molecules that are scattered at a sufficiently large angle to potentially hit the side of a particle is given by the fraction for which the scattering angle is $\geq \theta$, integrated over the 360° horizontal plane. This fraction (*F*) can be estimated using the cosine law for molecular scattering[62]

$$F = \cos^2\theta \qquad \text{(III)}$$

However, there are open spaces between particles that a molecule may pass through, even if scattered at a sufficiently large angle. To adjust for this, the fraction *F* scattered at angles $\geq \theta$ was reduced using the average dimensions of the particles and the average distance between them. The open dimensions were taken to be the part of the circumference of a circle drawn through the centers of four adjacent particles (Figure 7b) that is not covered by the four sides of the salt particles. This adjusted fraction is denoted as F'.

Incorporating the adjusted fraction F' and the top available surface area of the particles, the percentage of the geometric sample holder available for uptake and reaction can be estimated according to eq IV

$$\text{True reactive area} = A_{\text{top}} + (A_{\text{geom}} - A_{\text{top}}) \times F' \qquad \text{(IV)}$$

where A_{top} is the total surface area for the top of the salt particles, A_{geom} is the geometric surface area of the sample holder, and F' is the fraction of HNO_3 molecules striking a side of a NaCl particle after being scattered off the sample holder. This true reactive surface area was used to correct the geometric uptake coefficients (γ_{geom}) initially calculated using A_{geom}. These corrected values are reported as γ_{corr}.

Figure 6b shows the corrected uptake coefficients calculated in this manner at longer reaction times, γ_{corr}, as a function of the amount of salt on the holder for the experiments shown in Figure 6a. There is now no dependence on the fraction of a particle layer, as expected if the appropriate correction for the true available surface area is applied.

This treatment assumes that HNO_3 is not taken up irreversibly on the halocarbon wax as it hits a hole between salt particles. Consistent with this assumption, no uptake of HNO_3 was observed when the sample holder was exposed in the absence of salt. We note that this model is still applicable if HNO_3 has a finite lifetime on the surface before being released back into the gas phase.[63]

Table 2 summarizes the data for a range of particle sizes and number of NaCl particle layers at an initial HNO_3 concentration of $\sim 5 \times 10^{11}$ molecules cm^{-3}. The values for γ_{corr} are consistent, within experimental error, for both crushed and powder samples of all sizes. Although the crushed 164-μm particles have a more irregular shape (Figure 3) than the cubic, sieved powders (Figure 1), the agreement of the γ_{corr} values for crushed and cubic powders suggests that the method used for obtaining an average particle size for the crushed sample is appropriate. The average uptake coefficient, γ_{corr}, for all particle sizes is $(1.0 \pm 0.8) \times 10^{-3}$ (2s).

The initial uptake coefficient for HNO_3 when the lid is first opened is typically larger than that at longer reaction times. This can be seen in Figure 8, which shows a typical trend in the corrected uptake coefficients, γ_{corr}, as a function of reaction time. The larger uptake coefficient as $t \rightarrow 0$, γ^0_{corr}, is attributed to a lack of surface saturation at the short reaction times due to a fresh NaCl surface, void of product $NaNO_3$. As the reaction proceeds, the amount of nitrate product on the surface increases and the available reactive surface area decreases, leading to smaller values for the uptake coefficient, γ_{corr}. Under the conditions shown in Figure 4, complete surface saturation would be expected at 80 s for an uptake coefficient of $\sim 2 \times 10^{-3}$. However, the reaction clearly continues well beyond this time, in fact, decreases only slowly. This suggests that an approximately constant fraction of the initial surface continues to be available for reaction.

We present a model shown in Figure 9 that accounts for these observations and allows for an estimate of the fraction that continues to be available for reaction to be made. Previous Knudsen cell studies in this laboratory[19] established that SAW was present on the salt surface and played a role in preventing complete saturation of the NaCl surface. A variety of theoretical and experimental studies have established that SAW is likely

TABLE 2. Summary of HNO_3 Uptake Coefficients Corrected for the True Available Surface Area[a]

exp	particle size (μm)	mass (g)	no. of particle layers	$[HNO_3]_0$ (10^{11} mol cm^{-3})	γ_{corr} ($\pm$ 2s) (10^{-4})[b]	γ^0_{corr} ($\pm$ 2s) (10^{-3})	f_{SAW}
1	**164**	0.484	0.7	5.2	8.2 ± 0.9	4.6 ± 0.7	0.18
2		0.482	0.7	4.5	7.7 ± 0.6	1.4 ± 0.1	0.54
3		0.357	0.5	5.1	7.5 ± 0.5	1.2 ± 0.1	0.64
4		0.356	0.5	5.5	8.8 ± 1.3	3.7 ± 0.6	0.24
5		0.197	0.3	5.8	9.1 ± 0.5	1.6 ± 0.1	0.58
6		0.197	0.3	3.5	11.5 ± 0.8	1.7 ± 0.1	0.68
7		0.089	0.1	5.8	12.8 ± 0.5	2.2 ± 0.1	0.59
8		0.085	0.1	4.9	9.1 ± 0.2	2.7 ± 0.1	0.34
9	**177**	0.483	0.7	4.5	6.5 ± 0.7	3.4 ± 0.5	0.19
10		0.483	0.7	4.2	6.4 ± 2.0	3.3 ± 1.1	0.19
11		0.352	0.5	2.6	3.9 ± 0.7	2.0 ± 0.4	0.20
12		0.210	0.3	5.2	9.1 ± 0.7	1.5 ± 1.1	0.61
13		0.207	0.3	2.7	3.5 ± 0.4	1.3 ± 1.3	0.27
14		0.105	0.1	5.8	14.2 ± 0.4	2.7 ± 0.1	0.52
15		0.094	0.1	3.2	17.8 ± 0.8	1.9 ± 0.1	0.94
16	**290**	0.808	0.7	5.2	8.5 ± 0.5	1.3 ± 0.1	0.66
17		0.808	0.7	6.2	9.1 ± 0.7	3.4 ± 0.3	0.27
18		0.621	0.5	6.0	7.6 ± 0.4	1.7 ± 0.1	0.45
19		0.611	0.5	4.7	9.7 ± 0.6	1.3 ± 0.1	0.74
20		0.373	0.3	4.9	7.7 ± 0.7	1.0 ± 0.1	0.77
21		0.371	0.3	5.6	11.3 ± 0.7	1.3 ± 0.1	0.85
22		0.143	0.1	4.7	18.5 ± 0.4	2.9 ± 0.1	0.64
23		0.140	0.1	5.7	15.7 ± 0.3	1.8 ± 0.04	0.89
24	**439**	1.225	0.7	4.5	8.7 ± 0.9	2.3 ± 0.2	0.37
25		1.192	0.7	3.4	11.0 ± 0.8	2.6 ± 0.2	0.43
26		0.825	0.5	5.7	8.3 ± 0.4	2.0 ± 0.1	0.42
27		0.824	0.5	4.4	17.3 ± 3.0	3.2 ± 0.6	0.55
28		0.466	0.3	5.4	8.2 ± 0.7	1.1 ± 0.1	0.78
29		0.467	0.3	5.5	9.8 ± 0.4	1.6 ± 0.1	0.60
30		0.147	0.1	5.5	12.4 ± 0.2	3.6 ± 0.1	0.35
31		0.155	0.1	4.7	19.1 ± 0.3	3.7 ± 0.1	0.52
overall avg (2s):					**10.3 ± 8.0**	**2.3 ± 1.9**	**0.52 ± 0.44**

[a] A 3.9 mm aperture was used and all samples pumped on for several minutes; errors for individual runs are from a propagation of errors using the raw signals. [b] Calculated at the end of the third cycle of opening and closing the sample lid.

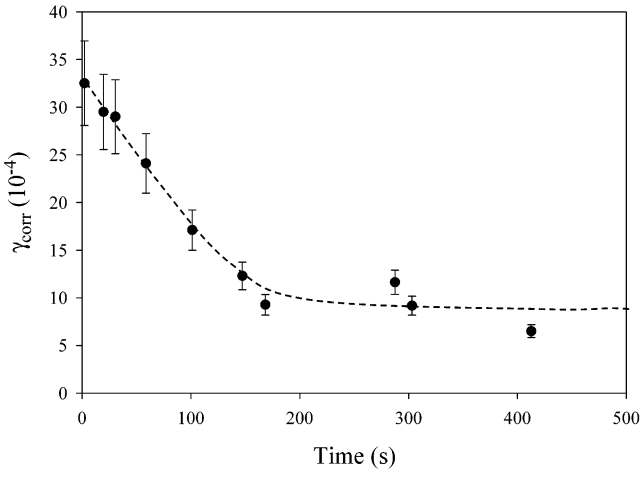

Figure 8. Typical decay in γ_{corr} with reaction time for uptake on 0.7 layers of 177 μm NaCl (experiment #9). Dotted line displays the general decrease in reaction probability with time, intended only as a guideline.

adsorbed at steps and edges of the NaCl surface. Oxygen in the water molecules likely bind to the sodium cation as depicted in Figure 9a. For example, Ahlswede and Jug[64] calculated that adsorption of water at a monatomic step is favored over that on the NaCl(100) terrace by about 10 kcal mol^{-1}. In the reaction of HNO_3 with NaCl, a chloride anion is replaced by a nitrate ion. If the reaction occurs close to a step or edge where SAW

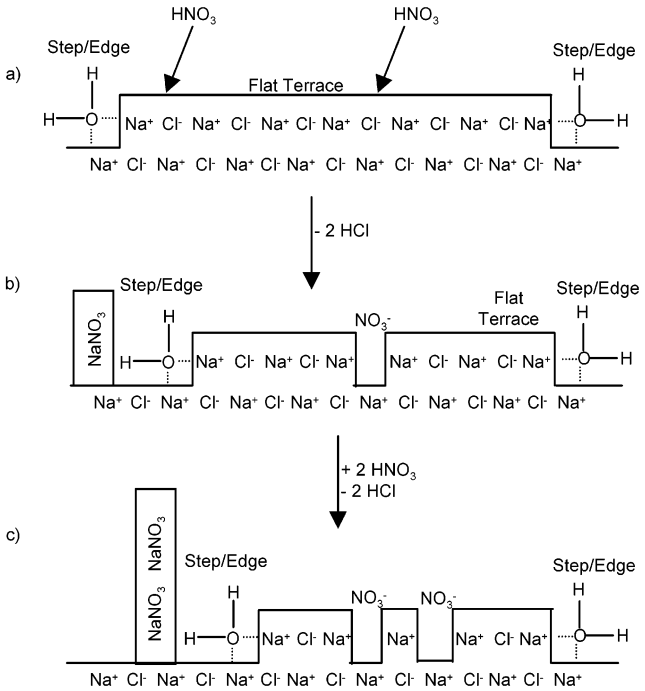

Figure 9. Schematic diagram of proposed model in which two types of reaction sites, flat terraces and SAW on edges and steps contribute to the uptake and reaction of HNO_3 on NaCl particles.

is available, the water can induce recrystallization of the nitrate from a thin film into regions of bulk crystalline $NaNO_3$ (Figure 9b). Water-induced mobilization of the surface ions and formation of microcrystallites of $NaNO_3$ on the NaCl surface has been observed by Hemminger and co-workers in which single-crystal NaCl(100) was reacted with HNO_3 and then exposed to water vapor.[65,66] This is also consistent with AFM observations of $NaNO_3$ "strings" along steps during the HNO_3–NaCl reaction.[34,67] Similarly, in infrared spectroscopic studies of the reactions of NaCl with HNO_3[35] and NO_2,[13] the asymmetric stretch of the nitrate ion appeared as a doublet. This splitting of the degeneracy to give two peaks was attributed to the formation of irregularly shaped microcrystallites of $NaNO_3$ in which longitudinal-transverse splitting of the degeneracy occurs due to the lowered symmetry.[35,68]

As the NaCl near the steps is converted to microcrystallites of $NaNO_3$, a new NaCl step is generated (Figure 9b). If SAW continues to be associated with these steps and edges, reaction along these new steps to form $NaNO_3$ would continue (Figure 9c). Such a mechanism would effectively lead to continuous reaction at the steps, with movement of the steps into the crystal, layer by layer. The surface would not become saturated as long as fresh NaCl steps continue to be generated.

However, if chloride ions at flat terrace sites remote from SAW are replaced by nitrate ions, mobilization of the surface ions and recrystallization into strings of $NaNO_3$ would not occur (Figure 9b). Such surface terrace sites will become saturated as the nitrate replaces surface chloride, in contrast to the situation at the steps and edges where SAW-assisted mobility of nitrate and the formation of $NaNO_3$ strings regenerates fresh NaCl.

Thus, the reaction may be treated as if it occurred at two different types of sites, one associated with SAW and one on terraces that are relatively free of SAW (dry). The measured uptake coefficient for HNO_3 may therefore be expressed as the sum of contributions from each type of site, weighted by the fraction of the surface associated with each type of site, f_{SAW}

and f_{dry}, respectively

$$\gamma_{meas} = f_{SAW}\,\gamma_{SAW} + f_{dry}\,\gamma_{dry} \quad \text{(V)}$$

For the SAW sites, we draw on the analysis of Ghosal and Hemminger,[31] in which an expression for the uptake coefficient as a function of the HNO_3 and SAW was developed

$$\gamma_{SAW} \propto \gamma^0 \frac{C}{[HNO_3] + C} \quad \text{(VI)}$$

where C is proportional to the amount of SAW.

In the limit of high SAW (large C) relative to HNO_3, sites are regenerated rapidly as the reaction occurs such that $\gamma_{SAW} \rightarrow \gamma^0$ with no dependence on the HNO_3 concentration. In our studies, no change in the initial uptake coefficient, γ^0, was observed over a range of HNO_3 concentrations from $(2-6) \times 10^{11}$ molecule cm^{-3}. Therefore, we assume that under these conditions for the SAW sites, regeneration of the surface to provide fresh NaCl is fast compared to the reaction, and γ_{SAW} is equal to γ^0 and is independent of time.

We assume that the value of the initial uptake coefficient is the same for the dry terrace sites. However, these terrace sites are not regenerated, and the uptake coefficient will decrease with time according to eq VII[48]

$$\gamma_{dry} = \gamma^0 e^{-at} \quad \text{(VII)}$$

where a is a constant that depends on the HNO_3 pressure

$$a = 3.51 \times 10^{16} \frac{\gamma^0 P}{N_s \sqrt{MT}} \quad \text{(VIII)}$$

P is the HNO_3 pressure in μTorr, N_s is the total number of dry terrace surface sites per cm^{-2}, M is the molecular weight in g mol^{-1}, and T is the temperature in K. With this relation, eq (V) can be rewritten as

$$\gamma_{meas} = f_{SAW}\gamma^0 + f_{dry}\gamma^0 e^{-at} \quad \text{(IX)}$$

in which $f_{SAW} + f_{dry} = 1$. As $t \rightarrow \infty$, $\gamma_{meas} \rightarrow f_{SAW}\,\gamma^0$ and as $t \rightarrow 0$, $\gamma_{meas} \rightarrow \gamma^0$. Therefore, the measured uptake coefficients at short reaction times can be used to obtain γ^0 for a fresh, unreacted NaCl surface. Those measured at longer reaction times can be used to obtain f_{SAW}, the average fraction of the surface that can be regenerated during the reaction due to the presence of SAW.

For each experiment, plots such as that in Figure 8 of the time-dependence of γ_{meas} were created, and values for γ^0 and f_{SAW} were obtained from the data at short and long reaction times, respectively. These values are summarized in Table 2. The overall average value of γ^0_{corr} is $(2.3 \pm 1.9) \times 10^{-3}$ (2s). Approximately 50% of the surface has sites that can be regenerated through the SAW-assisted mechanism [$f_{SAW} = 0.52 \pm 0.44$ (2s)], with the remaining half being terrace sites that become saturated during the reaction. Significant coverage of the surface by "strings" of product $NaNO_3$ has also been reported in AFM studies by Zangmeister and Pemberton[67] (although they used much higher concentrations of HNO_3 and H_2O vapor).

Previous studies of the HNO_3 uptake on fresh single-crystal NaCl(100)[8,31] or 500 μm NaCl crystals flattened against the walls of a flow tube[28] were analyzed[31] to give initial uptake coefficients of 1.3×10^{-3} and 1.1×10^{-3}, respectively. However, Ghosal and Hemminger[32] suggest that the value may be as large as 5×10^{-3}, depending on the nature of the NaCl surface, and hence, the amount of SAW. Our value of $\gamma^0 = (2.3 \pm 1.9) \times 10^{-3}$ (2s) is in excellent agreement with these studies. Our overall average uptake coefficient of all fractional layer experiments at longer reaction times [$\gamma_{corr} = (1.0 \pm 0.8) \times 10^{-3}$ (2s)], is smaller than γ^0, reflecting partial coverage of the reactive surface with $NaNO_3$ microcrystallites during the reaction. It is not clear how the larger uptake coefficients, $\sim (1-6) \times 10^{-2}$, obtained in some studies[29,34] can be reconciled with the uptake coefficient of $\sim 10^{-3}$ that is now found in this and two other studies using different techniques (Table 1).

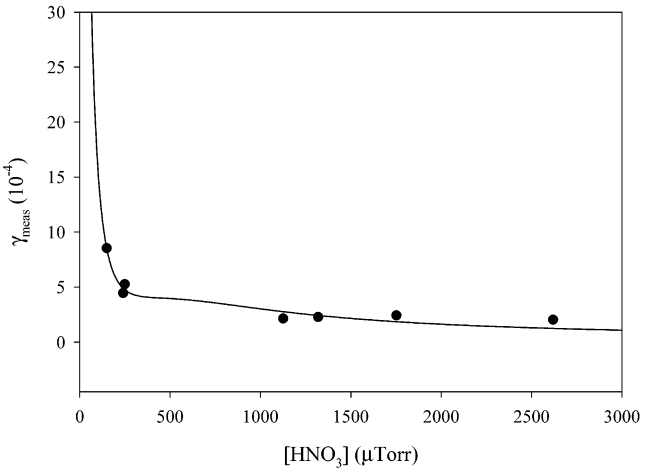

Figure 10. Corrected uptake coefficient (γ_{corr}) calculated at $t = 10$ s for varying HNO_3 concentrations on 0.5 layers of 290-μm NaCl particles.

The model developed here also predicts a dependence of the uptake coefficient on the HNO_3 concentration, which has been observed by Leu et al.[16] and Davies and Cox.[28] When $[HNO_3] \gg C$, eq VI predicts that the measured uptake coefficient for the SAW sites will depend inversely on HNO_3. On the basis of the Davies and Cox data on dry NaCl crystals, similar to those used here, in which the best fit[31] value for $C = 8 \times 10^{11}$, one would expect that for HNO_3 concentrations larger than the mid-10^{12} molecules cm^{-3} range, $\gamma_{SAW} \propto [HNO_3]^{-1}$.

The uptake coefficient for terrace sites, which can be saturated, has both a time dependence as discussed above, and a dependence on HNO_3 as expressed by Li et al.[48] eqs VII and VIII. For varying HNO_3 concentrations and at a particular reaction time, eq VII can be expressed as

$$\gamma_{dry} = \gamma^0 e^{-bP} \quad \text{(X)}$$

where

$$b = 3.51 \times 10^{16} \frac{\gamma^0 t}{N_s \sqrt{MT}} \quad \text{(XI)}$$

The dependence of γ_{meas} on HNO_3 at concentrations approaching 10^{14} molecules cm^{-3} will therefore have the following functional form for the combination of SAW and dry terrace sites

$$\gamma_{meas} = \frac{M}{[HNO_3]} + Pe^{-b[HNO_3]} \quad \text{(XII)}$$

In eq XII, M, P, and b are constants, and b is related to γ^0 via eq XI.

Figure 10 shows a plot of the measured uptake coefficients at a reaction time of 10 s as a function of the initial HNO_3

concentration for experiments with concentrations greater than mid-10^{12} molecule cm^{-3}, where eq XII should apply. The best fit to the data for eq XII gives a value for b of 0.0047, and from eq XI, $\gamma^0 = (1.1 \pm 0.4) \times 10^{-3}$ (2s). Given the assumptions, the agreement with the value obtained using the direct measurements at short reaction times of $(2.3 \pm 1.9) \times 10^{-3}$ (2s) is excellent.

Atmospheric Implications

Particles used in these studies contain steps, edges, and defects that clearly control the chemistry due to SAW. A similar situation is expected for sea salt aerosols. The value of the uptake coefficient at longer reaction times, $(1.0 \pm 0.8) \times 10^{-3}$ (2s), is most relevant to the reaction of gaseous HNO_3 with solid NaCl in the atmosphere under conditions where sea salt particles have effluoresced (e.g., upon being carried inland or to higher altitudes with lower relative humidities). The reaction of HNO_3 to generate photochemically inert HCl will compete with reactions of other oxides of nitrogen (reactions 2−3) that generate photochemically active chlorine-containing species. In a separate study under similar conditions conducted in this laboratory,[37] the uptake coefficient for the reaction of gaseous N_2O_5 with NaCl was found to be 2.9×10^{-3}, with a yield of ∼75% for $ClNO_2$. Taking typical concentrations of HNO_3 and N_2O_5 found in coastal urban areas as ∼100 ppt,[54,69,70] the reaction of HNO_3 with NaCl will be slower than the reaction of N_2O_5 with NaCl, which generates $ClNO_2$. This is contrary to that expected if the reaction probability of HNO_3 was on the order of 10^{-2} as suggested in several previous studies (Table 1).

It should be noted that this estimate of the relative importance of the HNO_3 and N_2O_5 reactions with sea salt aerosol will not apply to deliquesced sea salt particles in the MBL. The uptake of HNO_3 on aqueous NaCl solutions or deliquesced NaCl particles is fast, $\gamma = 0.2-0.5$,[26,27] while that of N_2O_5 is slower, $\gamma = 0.015-0.032$.[5,9,10,17,24,25] In the case of aqueous sea salt particles, the uptake and reaction of HNO_3 is expected to be more important than that of N_2O_5.

Acknowledgment. The authors gratefully thank the National Science Foundation (Grant # ATM-0079222) and the Department of Energy (Grant # DE-FG03-98 ER 62578) for support of this research, M. E. Gebel, J. Greaves, R. A. Cox and J. Mossinger for helpful discussions, and L. Moritz for technical assistance. We are particularly grateful to J. C. Hemminger for many stimulating discussions regarding this "simple" reaction.

References and Notes

(1) O'Dowd, C. D.; Smith, M. H.; Consterdine, I. E.; Lowe, J. A. *Atmos. Environ.* **1997**, *31*, 73.
(2) Finlayson-Pitts. *Nature* **1983**, *306*, 676.
(3) Finlayson-Pitts, B. J.; Ezell, M. J.; Pitts, J. N., Jr. *Nature* **1989**, *337*, 241.
(4) Behnke, W.; Zetzsch, C. *J. Aerosol Sci.* **1990**, *21*, S229.
(5) Behnke, W.; Kruger, H.-U.; Scheer, V.; Zetzsch, C. *J. Aerosol Sci.* **1991**, *22*, S609.
(6) Livingston, F. E.; Finlayson-Pitts, B. J. *Geophys. Res. Lett.* **1991**, *18*, 17.
(7) Behnke, W.; Scher, V.; Zetzsch, C. *J. Aerosol Sci.* **1993**, *24*, S115.
(8) Laux, J. M.; Hemminger, J. C.; Finlayson-Pitts, B. J. *Geophys. Res. Lett.* **1994**, *21*, 1623.
(9) George, C.; Ponche, J. L.; Mirabel, P.; Behnke, W.; Scheer, V.; Zetzsch, C. *J. Phys. Chem.* **1994**, *98*, 8780.
(10) Msibi, I. M.; Li, Y.; Schi, J. P.; Harrison, R. M. *J. Atmos. Chem.* **1994**, *18*, 291.
(11) Fenter, F. F.; Caloz, F.; Rossi, M. J. *J. Phys. Chem.* **1994**, *98*, 9801.
(12) Vogt, R.; Finlayson-Pitts, B. J. *Geophys. Res. Lett.* **1994**, *21*, 2291.
(13) Vogt, R.; Finlayson-Pitts, B. J. *J. Phys. Chem.* **1994**, *98*, 3747.
(14) Timonen, R. S.; Chu, L. T.; Leu, M. T.; Keyser, L. F. *J. Phys. Chem.* **1994**, *98*, 9509.
(15) Vogt, R.; Finlayson-Pitts, B. J. *J. Phys. Chem.* **1995**, *99*, 13052.
(16) Leu, M. T.; Timonen, R. S.; Keyser, L. F.; Yung, Y. L. *J. Phys. Chem.* **1995**, *99*, 13203.
(17) Zetzsch, C.; Behnke, W. *Ber. Bunsen-Ges. Phys. Chem.* **1992**, *96*, 488.
(18) Fenter, F. F.; Caloz, F.; Rossi, M. J. *J. Phys. Chem.* **1996**, *100*, 1008.
(19) Beichert, P.; Finlayson-Pitts, B. J. *J. Phys. Chem.* **1996**, *100*, 15218.
(20) Fenter, F. F.; Caloz, F.; Rossi, M. J. *Rev. Sci. Instrum.* **1997**, *68*, 3180.
(21) Ravishankara, A. R. *Science* **1997**, *276*, 1058.
(22) Andreae, M. O.; Crutzen, P. J. *Science* **1997**, *276*, 1052.
(23) Finlayson-Pitts, B. J.; Pitts, J. N. J. *Science* **1997**, *276*, 1045.
(24) Behnke, W.; George, C.; Scheer, V.; Zetzsch, C. *J. Geophys. Res.* **1997**, *102*, 3795.
(25) Schweitzer, F.; Mirabel, P.; George, C. *J. Phys. Chem. A* **1998**, *102*, 3942.
(26) Abbatt, J. P. D.; Waschewsky, G. C. G. *J. Phys. Chem. A* **1998**, *102*, 3719.
(27) ten Brink, H. M. *J. Aerosol Sci.* **1998**, *29*, 57.
(28) Davies, J. A.; Cox, R. A. *J. Phys. Chem. A* **1998**, *102*, 7631.
(29) Koch, T. G.; van den Bergh, H.; Rossi, M. J. *Phys. Chem. Chem. Phys.* **1999**, *1*, 2687.
(30) Hemminger, J. C. *Intern. Rev. Phys. Chem.* **1999**, *18*, 387.
(31) Ghosal, S.; Hemminger, J. C. *J. Phys. Chem. A* **1999**, *103*, 4777.
(32) Ghosal, S.; Hemminger, J. C. *J. Phys. Chem. A* **2003**, submitted for publication.
(33) Finlayson-Pitts, B. J.; Hemminger, J. C. *J. Phys. Chem. A* **2000**, *104*, 11463.
(34) Zangmeister, C. D.; Pemberton, J. E. *J. Phys. Chem. A* **2001**, *105*, 3788.
(35) Sporleder, D.; Ewing, G. E. *J. Phys. Chem. A* **2001**, *105*, 1838.
(36) Guimbaud, C.; Arens, F.; Gutzwiller, L.; Gaggeler, H. W.; Ammann, M. *Atmos. Chem. Phys. Discuss.* **2002**, *2*, 739.
(37) Hoffman, R. C.; Gebel, M. E.; Fox, B. S.; Finlayson-Pitts, B. J. *Phys. Chem. Chem. Phys.* **2003**, *5*, 1780.
(38) Junge, C. E. *Tellus* **1956**, *8*, 127.
(39) Moyers, J. L.; Duce, R. A. *J. Geophys. Res.* **1972**, *77*, 5330.
(40) Keene, W. C.; Pszenny, A. A.; Jacob, D. J.; Duce, R. A.; Galloway, J. N.; Schultz-Tokos, J. J.; Sievering, H.; Boatman, J. F. *Global Biochem. Cycles* **1990**, *4*, 407.
(41) Mouri, H.; Okada, K. *Geophys. Res. Lett.* **1993**, *20*, 49.
(42) McInnes, L. M.; Covert, D. S.; Quinn, P. K.; Germani, M. S. *J. Geophys. Res.* **1994**, *99*, 8257.
(43) Laskin, A.; Iedema, M. J.; Cowin, J. P. *Environ. Sci. Technol.* **2002**, *36*, 4948.
(44) Rogaski, C. A.; Golden, D. M.; Williams, L. R. *Geophys. Res. Lett.* **1997**, *24*, 381.
(45) Goodman, A. L.; Underwood, G. M.; Grassian, V. H. *J. Geophys. Res.* **2000**, *105*, 29053.
(46) Underwood, G. M.; Li, P.; Usher, C. R.; Grassian, V. H. *J. Phys. Chem. A* **2000**, *104*, 819.
(47) Underwood, G. M.; Li, P.; Al-Abadleh, H.; Grassian, V. H. *J. Phys. Chem. A* **2001**, *105*, 6609.
(48) Li, P.; Al-Abadleh, H. A.; Grassian, V. H. *J. Phys. Chem. A* **2002**, *106*, 1210.
(49) DeHaan, D. O.; Finlayson-Pitts, B. J. *J. Phys. Chem. A* **1997**, *101*, 9993.
(50) Gebel, M. E.; Finlayson-Pitts, B. J. *J. Phys. Chem. A* **2001**, *105*, 5178.
(51) Golden, D. M.; Spokes, G. N.; Benson, S. W. *Angew. Chem., Int. Ed. Engl.* **1973**, *12*, 534.
(52) Quinlan, M. A.; Reihs, C. M.; Golden, D. M.; Tolbert, M. A. *J. Phys. Chem.* **1990**, *94*, 3255.
(53) Caloz, F.; Fenter, F. F.; Tabor, K. D.; Rossi, M. J. *Rev. Sci. Instr.* **1997**, *68*, 3172.
(54) Finlayson-Pitts, B. J.; Pitts, J. N. Jr. *Chemistry of the Upper and Lower Atmosphere − Theory, Experiments, and Applications*; Academic Press: San Diego, 2000.
(55) Barraclough, P. B.; Hall, P. G. *Surf. Sci.* **1974**, *46*, 393.
(56) Smart, R. S. C.; Sheppard, N. *J. Chem. Soc., Faraday Trans. 2* **1976**, *72*, 707.
(57) Estel, J.; Hoinkes, H.; Kaarmann, H.; Nahr, H.; Wilsch, H. *Surf. Sci.* **1976**, *54*, 393.
(58) Folsch, S.; Henzler, M. *Surf. Sci.* **1991**, *247*, 269.
(59) Wassermann, B.; Mirbt, S.; Reif, J.; Zink, J. C.; Matthias, E. *J. Chem. Phys.* **1993**, *98*, 10049.
(60) Dai, D. J.; Ewing, G. E. *J. Chem. Phys.* **1993**, *98*, 5050.
(61) Dai, D. J.; Peters, S. J.; Ewing, G. E. *J. Phys. Chem.* **1995**, *99*, 10299.
(62) Boeckmann, M. D. *J. Vac. Sci. Technol. A* **1986**, *4*, 353.
(63) Head-Gordon, M.; Tully, J. C.; Rettner, C. T.; Mullins, C. B. *J. Chem. Phys.* **1991**, *94*, 1516.
(64) Ahlswede, B.; Jug, K. *Surf. Sci.* **1999**, *4.9*, 86.

(65) Allen, H. C.; Laux, J. M.; Vogt, R.; Finlayson-Pitts, B. J.; Hemminger, J. C. *J. Phys. Chem.* **1996**, *100*, 6371.
(66) Laux, J. M.; Fister, T. F.; Finlayson-Pitts, B. J.; Hemminger, J. C. *J. Phys. Chem.* **1996**, *100*, 19891.
(67) Zangmeister, C. D.; Pemberton, J. E. *J. Phys. Chem. B* **1998**, *102*, 8950.
(68) Rowland, B.; Kadagathur, N. S.; Devlin, J. P. *J. Chem. Phys.* **1995**, *102*, 13.
(69) Atkinson, R.; Winer, A. M.; Pitts, J., J. N. *Atmos. Environ.* **1986**, *20*, 331.
(70) Brown, S. S.; Stark, H.; Ciciora, S. J.; Ravishankara, A. R. *Geophys. Res. Lett.* **2001**, *28*, 3227.
(71) Keyser, L. F.; Moore, S. B.; Leu, M.-T. *J. Phys. Chem.* **1991**, *95*, 5496.
(72) Keyser, L. F.; Leu, M.-T.; Moore, S. B. *J. Phys. Chem.* **1993**, *97*, 2800.